

Supplementary Materials for
**Rapid recruitment and IFN- γ -mediated activation of monocytes dictate focal
radiotherapy efficacy**

Sirimuvva Tadepalli *et al.*

Corresponding author: Juliana Idoyaga, jidoyaga@stanford.edu

Sci. Immunol. **8**, eadd7446 (2023)
DOI: 10.1126/sciimmunol.add7446

The PDF file includes:

Supplementary Materials and Methods
Figs. S1 to S8
Tables S1 to S7
References (89–91)

Other Supplementary Material for this manuscript includes the following:

Data file S1
MDAR Reproducibility Report

SUPPLEMENTARY MATERIALS

SUPPLEMENTARY MATERIAL AND METHODS

Imaging for CRT and SRT-like

CRT- and SRT-like-treated animals were imaged using 400 x-ray beams of energy 40 kVp and current 0.5 mA spaced over 360 degrees, allowing reconstruction of volumetric CT images at a voxel resolution of 0.4 x 0.4 x 0.4 mm. These images were then used to prescribe a radiation treatment to the animal consisting of either 2 anti-parallel beams (CRT) or a single beam (one beam CRT and SRT-like). These beams were collimated to a width of 1 cm at isocenter and prescribed to deliver a cumulative dose of 20Gy or 8Gy at isocenter. CRT treatments delivered radiation beams designed to target the subcutaneous tumor while avoiding as much underlying tissue as possible. SRT-like treatments targeted a mouse that had been positioned with its tumor protruding through a 1 cm hole in a sheet of acrylic, to mimic radiation treatments delivered for SRT. SRT-like exhibited falloff in dose with distance from the source (mean dose 20.0Gy, ranging 19.5-20.4Gy). Importantly, SRT-like resulted in significant radiation doses to normal tissues, including intestine and kidney (ranging from 16.0-18.4Gy).

RT machine calibration

Calibration of both the X-Rad SmART and the Polaris were performed quarterly using both ion chamber and film dosimetry. Half value layers were measured for these treatment beams of 1.16 mm Cu (X-Rad SmART) and 1.08 mm Cu (Polaris). For both systems, a PTW Farmer Ionization chamber was used to measure exposure in air, calculated dose rate using AAPM report TG-61 (89). Radiochromic film dosimetry was used to measure the output factors for specific shield setups relative to an open field. In addition, film dosimetry was used to assess the dose delivered outside the radiation beam for both the X-Rad SmART and the Polaris setups. In both cases, the measured dose outside the beam aperture was less than 1% of the prescribed dose.

Western blot analysis

Tumor harvested and lysed using RIPA buffer: 25 mM Tris–HCl pH 7.6, 1% NP-40, 1% sodium-deoxycholate, 150 mM NaCl, 0.1% sodium dodecyl sulfate (SDS), and cOmplete™ EDTA-free protease inhibitor cocktail (1 tablet per 50ml of solution). Protein lysates were sonicated and mechanically disrupted with a 26-gauge needle. Protein concentration was determined using the Pierce™ BCA protein assay kit (ThermoFisher Scientific). Protein samples (25 µg/lane) were boiled for 5 min in protein loading buffer Blue (National Diagnostics) and loaded on a 10% SDS–PAGE gel. Following electrophoresis, proteins were transferred onto PVDF membrane (GVS North America), blocked in 1% milk in PBS-T (PBS with 0.1% Tween) (Fisher Scientific). Primary antibodies against STING (D2P2F; Rabbit mAb #13647, Cell Signaling) and β3-Tubulin (D65A4; XP® Rabbit mAb #5666, Cell Signaling) were added to the membrane and incubated overnight at 4 °C. Secondary antibody goat anti-rabbit-HRP (GeneTex; 1:10000 dilution) was added for 1 h at room temperature. Blots were scanned with the BioRad Chemidoc™MP to visualize protein signals and intensities.

Antibiotic treatment

An antibiotic cocktail containing 1g/L Ampicillin (Fisher Scientific), 0.5g/L Vancomycin (Fisher Scientific), 1 g/L Neomycin (Fisher Scientific), 0.5 g/L Metronidazole (MP Biomedical LLC), and 10g/L Splenda was administered to tumor bearing mice *ad libitum* 3-days prior RT and replenished with new solution every 3-4 days until humane endpoint. Antibiotic efficacy was confirmed by testing the growth of bacterial colonies from stool.

STING knockout MC38 cell line generation

A STING knockout MC38 cell line (MC38^{ΔSTING}) was generated using CRISPR-Cas9. gRNA Oligos (**Table S6**; Integrated DNA Technologies) were cloned into the Cas9-expressing pX458 gRNA plasmid (Addgene #48138) using Zhang Lab target sequence-cloning protocol (<https://www.addgene.org/crispr/zhang/>). The cloning product was transfected into MC38 using

Lipofectamine 3000 (ThermoFisher) according to the manufacturer's guidelines. GFP⁺ cells were single cell sorted 48 hrs post-transfection, expanded and analyzed by Sanger sequencing. Sanger data files and sgRNA target sequences were input into Inference of CRISPR Edits (ICE) analysis (<https://ice.synthego.com>) to determine editing efficiency and quantify generated indels. A subclone with a homozygous 1-bp deletion was chosen for experiments (**fig. S6C-E**).

SUPPLEMENTARY FIGURES

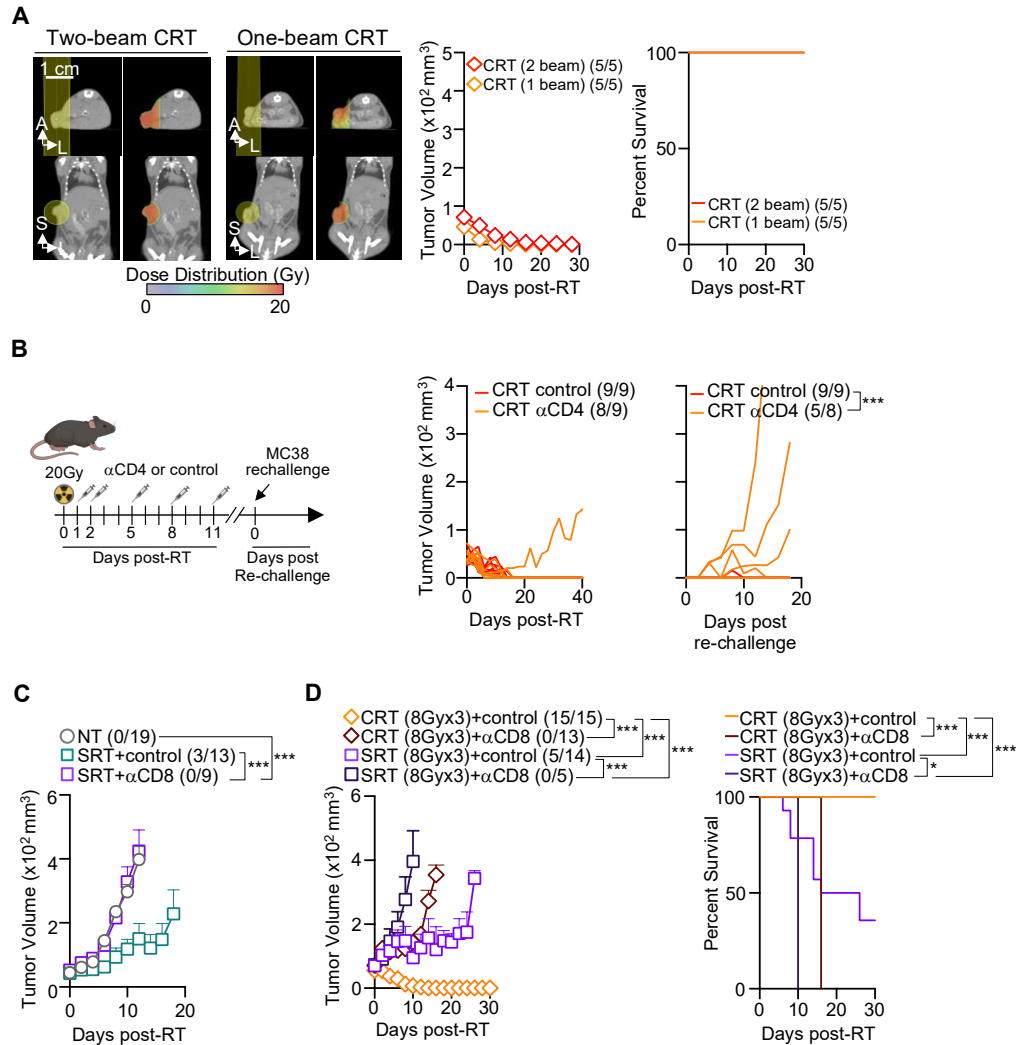


fig. S1. T cells influence RT outcome, independently of the fractionation or delivery mode.

(A) (Left) CT scans showing radiation beam orientation following two- and one-beam CRT. (Middle) Mean tumor growth + SEM with ratio of surviving mice in parenthesis. (Right) Survival curve of either one- or two-beam CRT ($n=5/\text{group}$, 1 exp.). **(B)** MC38-bearing mice post-CRT and 200 μg αCD4 /control Ab. (Left) Experimental design. (Middle) Individual mouse primary tumor growth. (Right) Individual mouse tumor growth following re-challenged with MC38 cells 50-days post-RT ($n=8-9/\text{group}$, 2 exp.). **(C)** Mean tumor growth + SEM of MC38-bearing mice post-SRT and 200 μg αCD8 /control Ab ($n=9-19/\text{group}$, 2-4 exp.). Ratio of surviving mice is noted in parenthesis. **(D)** MC38-bearing mice following 8Gyx3 RT and 200 μg αCD8 /control Ab. (Left) Mean tumor growth + SEM with ratio of surviving mice in parenthesis. (Right) Survival curve ($n=5-15/\text{group}$, 1-3 exp.). Statistics: Two-way ANOVA plus Tukey's post-hoc test for mean tumor growth (**A-D**), and Mantel-Cox test for survival curves (**A, D**).

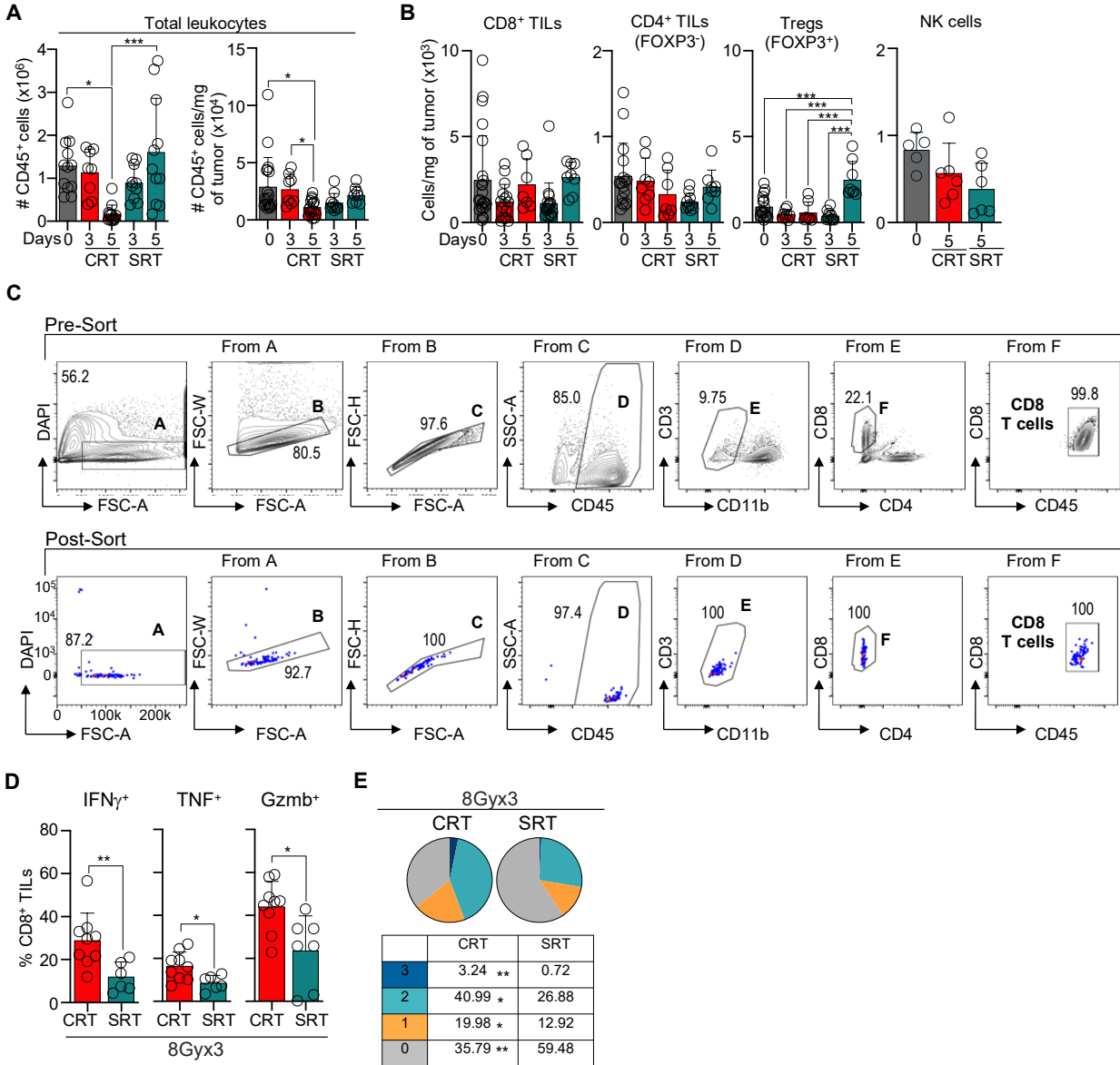


fig. S2. CD8⁺ TIL analysis post-RT. (A-B) MC38-bearing mice 1-5 days post-RT or NT controls (n=5-16/group, 3-6 exp). (A) Number (left) and cells/mg of tumor (right) of CD45⁺ cells. (B) Number of lymphocyte/mg of tumor. (C) CD8⁺ TILs from MC38-bearing mice 3-days post-RT vs NT controls were sorted for NanoString analysis. (Top) Representative gating strategy and (bottom) post-sort purity. (D-E) MC38-bearing mice 3-days post- 8Gyx3 RT. (D) Frequency of CD8⁺ TILs producing IFN γ , TNF, and Gzmb, by flow cytometry (n=6-9/group, 3 exp.). (E) Boolean analyses of CD8⁺ TILs producing 1, 2 or 3 effector molecules (n=6-9/group, 3 exp.). Statistics: One-way ANOVA plus Tukey's post-hoc test (A-B, E); Unpaired t-test (D).

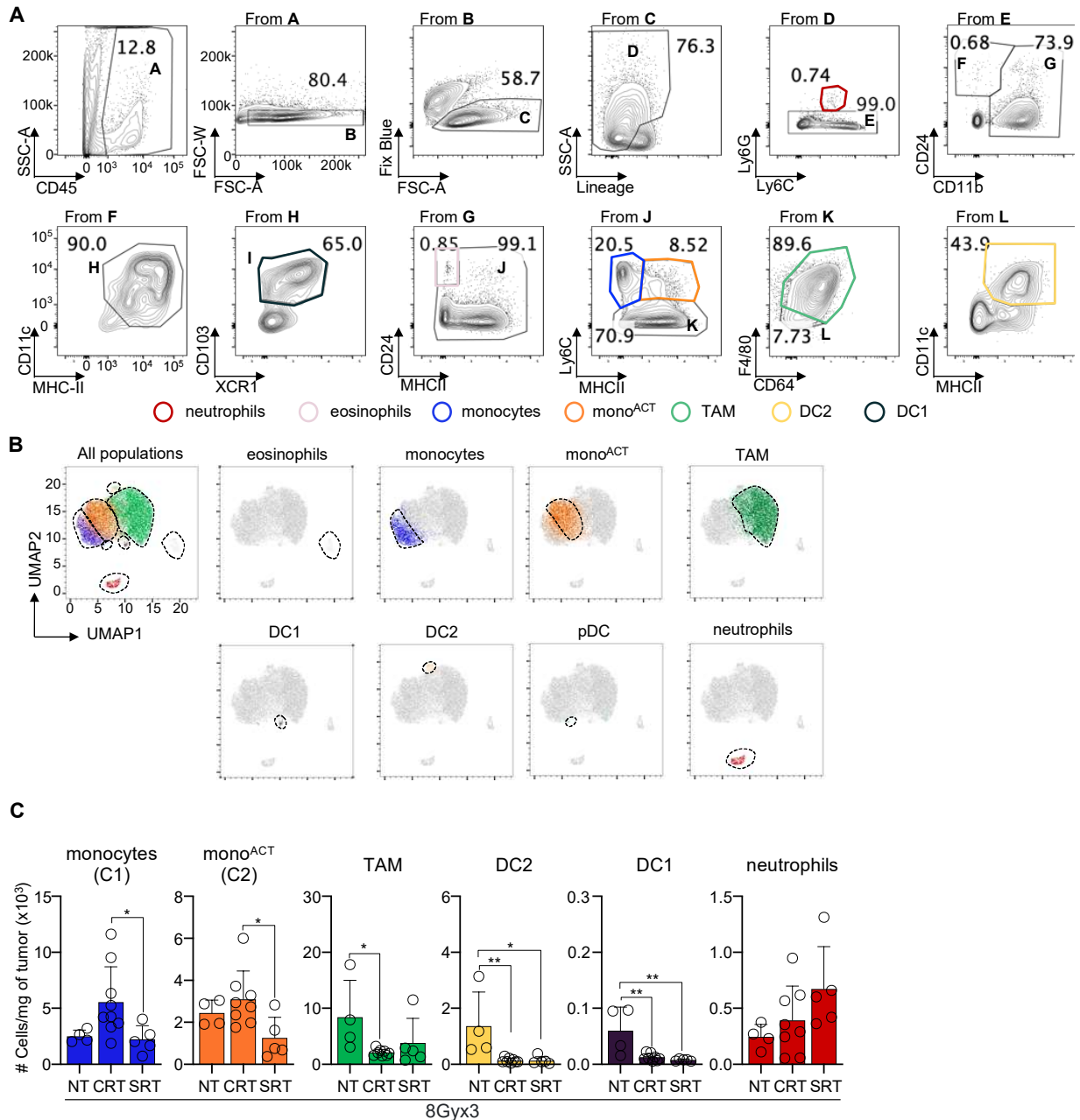


fig. S3. Myeloid cell analysis post-RT. (A-B) MC38-bearing mice 1- and 5-days post-RT or NT, by CyTOF. (A) Myeloid cell gating strategy based on unbiased X-shift analysis using K-nearest neighbor density estimation. Lineage staining includes CD3⁺, CD19⁺, and NK1.1⁺ cells. (B) Myeloid cells gated as in (A), and overlaid in the unbiased UMAP generated by CyTOF analysis shown in Fig. 3A (n=3/group, 2 exp.). (C) Cells/mg of 3-days post- 8Gyx3 RT (n=4-8/group, 2-3 exp.). Statistics: One-way ANOVA plus Tukey's post-hoc test.

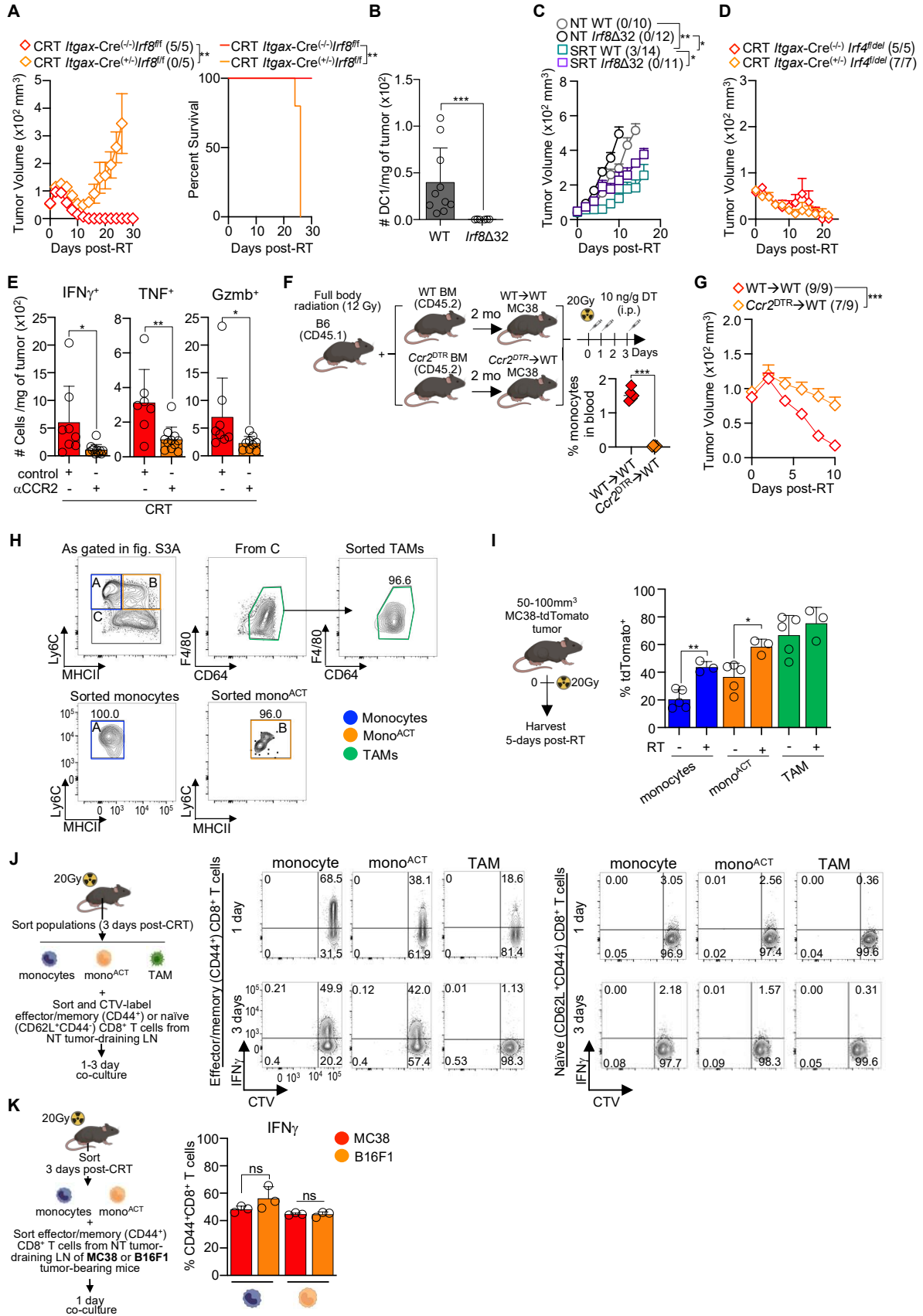


fig. S4. Role of DC1, DC2, and monocyte post-RT. (A) MC38-bearing *Itgax-Cre^{+/-} xIrf8^{ff}* or *Itgax-Cre^{-/-} xIrf8^{ff}* mice post-CRT (n=5/group, 1 exp.). (Left) Mean tumor growth + SEM with ratio of surviving mice in parenthesis. (Right) Survival curves. (B) Number of DC1/mg of tumor 3-days post-CRT in WT or *Irf8Δ32* mice. (C) Mean tumor growth + SEM of MC38-bearing WT or *Irf8Δ32* mice post-SRT with ratio of surviving mice in parenthesis (n=10-14/group, 2-3 exp.). (D) Mean tumor growth + SEM of MC38-bearing *Itgax-Cre^{+/-} xIrf4^{fl/del}* or *Itgax-Cre^{-/-} xIrf4^{fl/del}* mice post-CRT with ratio of surviving mice in parenthesis (n=5-7/group, 2 exp.). (E) Number of CD8⁺ TILs/mg of tumor producing IFN γ , TNF, and GzmB, from MC38-bearing mice 3-days post-CRT and α Ccr2/control Ab, by flow cytometry (n=7-8/group, 2-3 exp.). (F-G) BMC were generated by transplanting WT or *Ccr2^{DTR}* BM into lethally irradiated mice. Two months post-transplantation, MC38 tumors were engrafted, CRT-treated, and inoculated with diphtheria toxin (DT) administered i.p (10ng/g) on 0, 1-, and 3-days (n=9/group, 2 exp.). (F) Blood monocyte frequency following DT inoculation 3-days post-RT, by flow cytometry. (G) Mean tumor volume + SEM within the first 10 days post-CRT with ratio of surviving mice in parenthesis (n=9/group, 2 exp.). (H) Sorting strategy and purity of monocytes, mono^{ACT}, and TAM 3-days post-RT from MC38-bearing mice (1 of 8 exp.). Cells were gated as in **fig.S3A**. (I) MC38^{tdTomato} tumors were analyzed for the expression tumor antigen (tdTomato⁺) in myeloid cells 5-days post-CRT, by flow cytometry (n=3-4/group, 2 exp.). (J) Myeloid cells sorted 3-days post-CRT were co-cultured *ex vivo* with effector/memory (CD44⁺) or naïve (CD44⁻CD62L⁺) CTV-labeled CD8⁺ T cells obtained from MC38-tumor draining LN. (Left) Experimental design. (Right) Representative flow cytometry experiment (n=3-5/group, 3 exp.). (K) As in (J), but CD44⁺CD8⁺ T cells were obtained from MC38 or B16F1 tumor-draining LN and cultured with monocytes or mono^{ACT} sorted from MC38 tumors 3-days post-RT (n=3/group, 2 exp.). Statistics: Two-way ANOVA plus Tukey's post-hoc test for mean tumor growth (A, C, D, G); Mantel-Cox test for survival curves (A); Unpaired t-test (B, E-F); One-way ANOVA plus Tukey's post-hoc test (I, K).

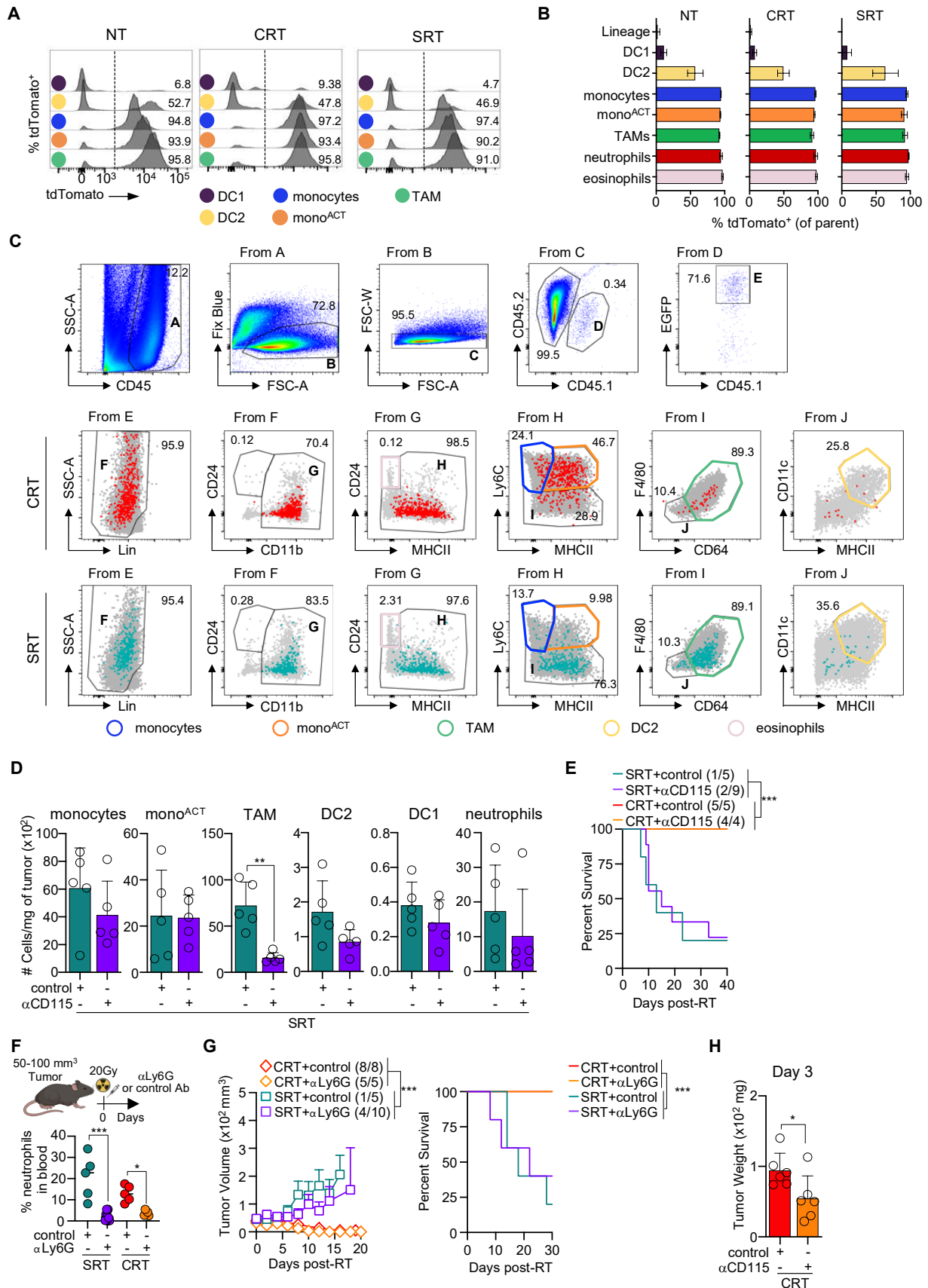


fig. S5. Myeloid cell fate and contribution to RT efficacy. (A-B) MC38-bearing *Ms4a3^{tdTomato}* mice 5-days post-RT or NT (n=3-4/group, 2-3 exp.). **(A)** Representative histograms showing tdTomato expression in each cell population, by flow cytometry. **(B)** As in A, but percentage of tdTomato⁺ cells per population. **(C)** BM CD45.1 monocytes from *Cx3cr1^{EGFP}* mice were negatively enriched and adoptively transferred into MC38-bearing B6 (CD45.2) mice 1-2 hrs post-CRT. (Top) Gating strategy to identified CD45.1 adoptively transferred cells in tumors, by flow cytometry. (Middle and bottom) Phenotype of donor CD45.1 cells from CRT (red) and SRT (teal) tumors overlaid over CD45.2 host cells (gray). **(D-E)** MC38-bearing mice post-RT and α CD115/control Ab inoculation. **(D)** Cell number/mg tumor 3-days post-SRT (n=5/group, 2 exp.). **(E)** Survival curve with ratio of surviving mice in parentheses (n=5/group, 2 exp.). **(F-G)** MC38-bearing mice post-RT and one dose of 200 μ g α Ly6G/control Ab the day of RT. **(F)** Blood neutrophil frequency 2-days post-RT (n=5-10/group, 2 exp.) **(G)** (Left) Mean tumor growth + SEM curves with ratio of surviving mice in parenthesis. (Right) Survival curve. **(H)** As in D, tumor weight (mg) 3-days post-CRT (n=6/group, 2-3 exp.). Statistics: Unpaired t-test (**D, H**); Mantel-Cox test for survival curves (**E, G**); One-way ANOVA plus Tukey's post-hoc test (**F**); Two-way ANOVA plus Tukey's post-hoc test for mean tumor growth (**G**).

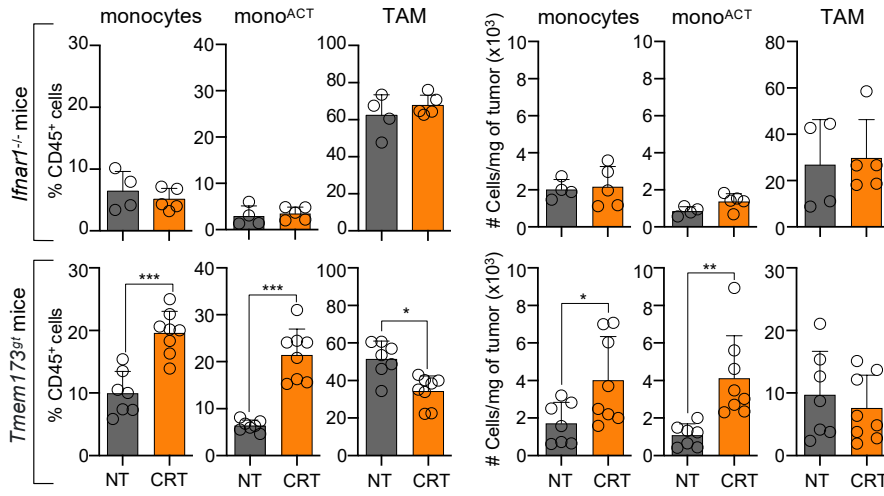
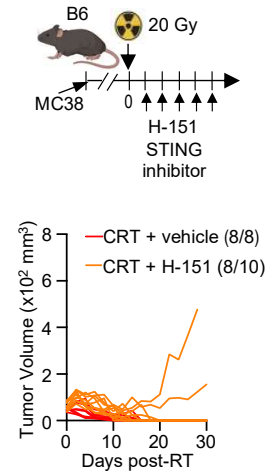
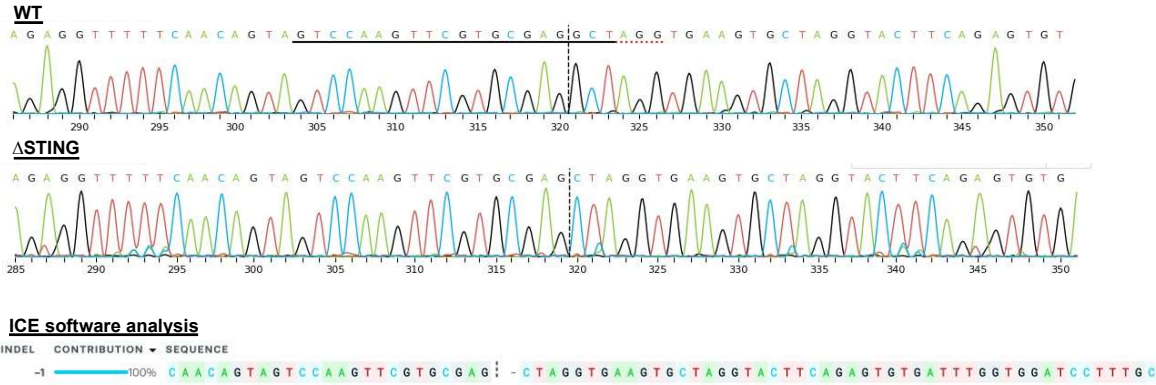
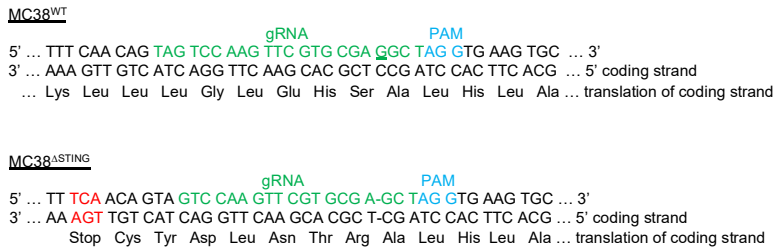
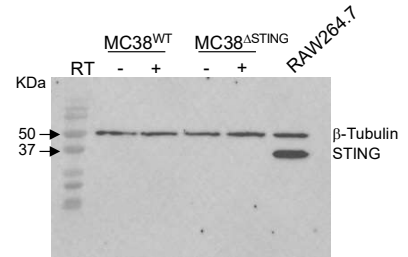
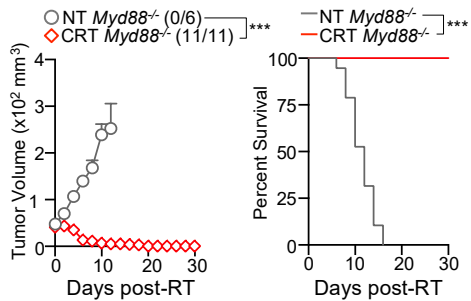
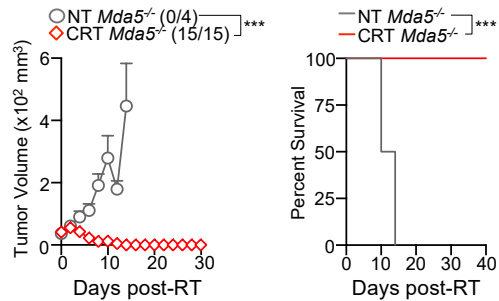
A**B****C****D****E****F****G**

fig. S6. CRT-mediated immune response is independent of STING, MyD88 and MDA5. (A) MC38-bearing *Ifnar1^{-/-}* and *Tmem173^{gt}* mice 3-days post-CRT. Shown are myeloid cell frequencies (left) and numbers/mg of tumor (right), by flow cytometry (n=4-8/group, 2-3 exp.). **(B)** Individual tumor growth curves of MC38-bearing mice post-CRT, with STING inhibitor H-151 or vehicle (inoculated 1-5 days post-RT) (n=8-10/group, 2 exp.). **(C)** Sanger sequencing chromatograms of MC38^{WT} and MC38^{ASTING} cell clones. Line depicts gRNA position (above). Protospacer-adjacent motif (PAM) is marked with red dashed line. ICE software analysis of Sanger sequencing data confirmed a homozygous 1bp deletion in the MC38^{ASTING} cell (below). **(D)** Predicted effect at DNA and protein levels following 1bp deletion in the MC38^{ASTING}. gRNA, PAM and premature stop codon are shown in green, blue and red, respectively. **(E)** MC38^{WT} and MC38^{ASTING} cells were analyzed for the expression of STING, by Western blot. Cells were left untreated (NT) or treated with 20Gy radiation *in vitro* followed by 24 hrs culture. β -Tubulin was used as the loading control. RAW264.7 cells were used as positive control for STING expression. One representative experiment of 3 is shown. **(F-G)** MC38-bearing *Myd88^{-/-}* and *Mda5^{-/-}* post-CRT vs NT (n=4-15/group, 2-3 exp.). (Left panels) Mean tumor growth + SEM with ratios of surviving mice in parenthesis. (Right panels) Survival curves. Statistics: Unpaired t-test **(A)**; Two-way ANOVA plus Tukey's post-hoc test for tumor growth curves **(B, F, G)**; Mantel-Cox test for survival curves **(F, G)**.

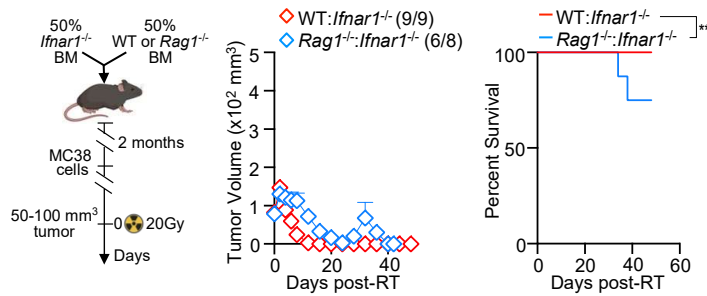


fig. S7. CRT-mediated immune response is only partially dependent on IFN-I signaling in T cells.

BMC were generated by the transplanting 50% *Ifnar1*^{-/-} BM and 50% WT or *Rag1*^{-/-} BM into lethally irradiated CD45.1 mice. Transplantation was established for 2 months prior to MC38 engraftment and CRT treatment. (Left) Experimental design. (Middle) Mean tumor volume + SEM with ratios of surviving mice in parenthesis. (Right) Survival curve (n=8-9/group, 2 exp.). Statistics: Two-way ANOVA plus Tukey's post-hoc test for mean tumor growth curves; Mantel-Cox test for survival curves.

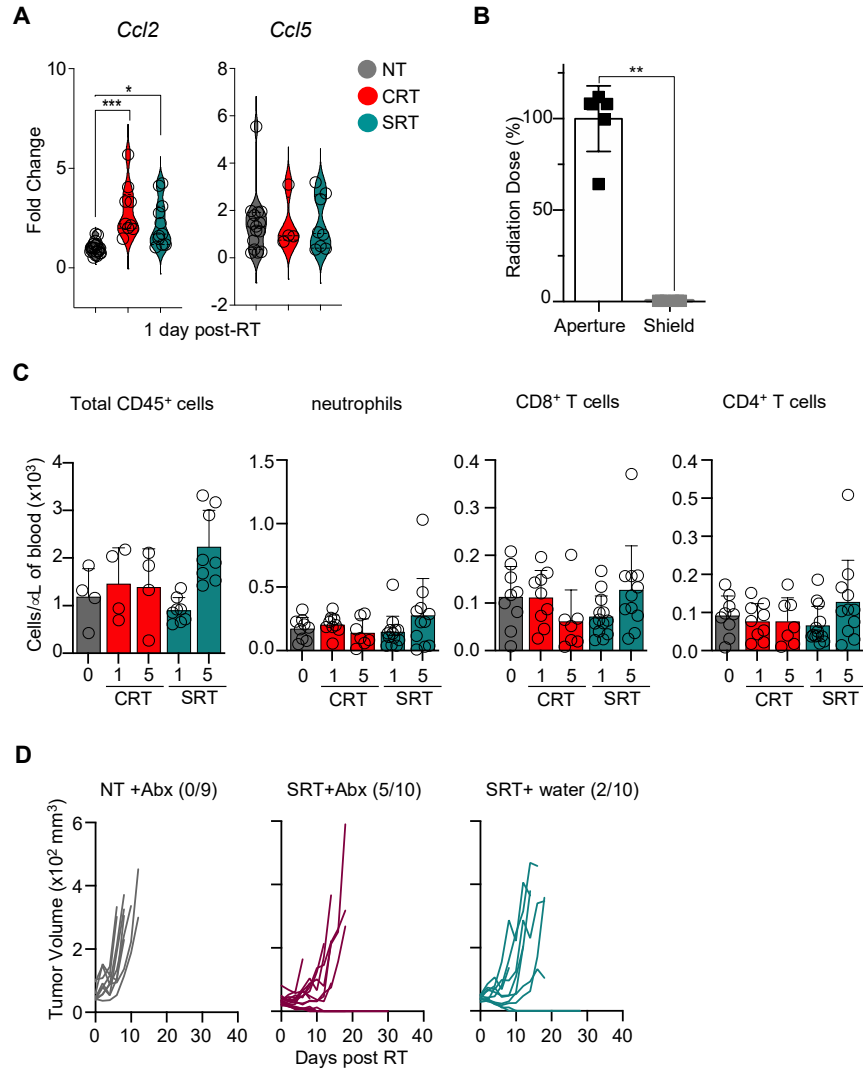


fig. S8. SRT does not promote systemic radiation toxicity. (A) Tumors from MC38-bearing mice were analyzed 1-day post-RT for the expression of *Ccl2* and *Ccl5*, by qPCR (n=4-17/group, 2-3 exp). (B) Radiation dose (relative percent change) measured through the aperture and behind the lead shield using radio-chromic film dosimeter (Gafchromic EBT-3 film) (n=6/group, 1 exp.). (C) MC38-bearing mice post-RT. CD45⁺ cells, neutrophils, CD8⁺ and CD4⁺ T cells 1- and 5-days post-RT per μ L of blood (n=4-13/group, 2-3 exp.). (D) MC38-bearing mice post-SRT and oral antibiotic cocktail treatment. Individual mouse tumor growth curves with ratio of surviving mice in parentheses (n=9-10/group, 2-3 exp.). Statistics: One-way ANOVA plus Tukey's post-hoc test (A,C); Unpaired t-test (B); Two-way ANOVA plus Tukey's post-hoc test for tumor growth curves (D).

SUPPLEMENTARY TABLES

Table S1. List of animals

Mouse Strain with common names in parenthesis	Origin
C57BL/6J (B6)	Jackson laboratory (Jax#000664)
<i>Tmem173^{gt}</i>	Jackson laboratory (Jax#017537)
<i>Braf^{CA} x Pten^{flf} x Tyr^{CreER}</i> (BRaf/Pten)	Jackson laboratory (Jax#013590)
<i>Ccr2^{-/-}</i>	Jackson laboratory (Jax#004999)
<i>Rag1^{-/-}</i>	Jackson laboratory (Jax#002216)
<i>Itgax-Cre</i>	Jackson laboratory (Jax#008068)
<i>Irf4^{flf}</i>	Jackson laboratory (Jax#009380)
<i>Irf8^{flf}</i>	Jackson laboratory (Jax#014175)
<i>Lyz2^{Cre}</i>	Jackson laboratory (Jax#004781)
<i>Csf1r^{LSL-DTR}</i>	Jackson laboratory (Jax#024046)
<i>Ifnb1^{EYFP}</i> (<i>Ifnb^{mob}</i>)	Jackson laboratory (Jax#010818)
<i>Ifnar1^{-/-}</i>	Jackson laboratory (Jax#032045)
<i>Foxp3^{DTR}</i>	Jackson laboratory (Jax#016958)
<i>Cx3cr1^{EGFP}</i>	Jackson laboratory (Jax#008451)
<i>Myd88^{-/-}</i>	Jackson laboratory (Jax#009088)
<i>Mda5^{-/-}</i>	Jackson laboratory (Jax#015812)
Ai9(RCL-tdT) (<i>Rosa^{LSL-tdTomato}</i>)	Jackson laboratory (Jax#007905)
B6-Ly5.1/Cr (CD45.1)	Charles River (Cat#564)
<i>Irf8Δ32</i>	Jackson laboratory (Jax#032744)
<i>Ccr2^{DTR}</i>	Obtained from Dr. Lavine (54)
<i>Ms4a3^{Cre}</i>	Obtained from Dr. Ginhoux (56)
<i>Ms4a3^{Cre} x Rosa^{LSL-tdTomato}</i>	In-house breeding (56)
<i>Itgax-Cre x Irf8^{flf}</i>	In-house breeding (48)
<i>Itgax-Cre x Irf4^{flf/del} **</i>	In-house breeding (52)
<i>Lyz2^{Cre} x Csf1r^{LSL-DTR}</i> (MM ^{DTR})	In-house breeding(55)

**As previously reported, this mouse strain frequently generates germline deletions, which were detected by genotyping (53). Although we did not detect immunological differences, all our experiments included *Irf4^{flf}* and *Irf4^{flf/del}* mice as controls.

Table S2. List of cell lines

List of cell-lines used for *in vivo* and *in vitro* experiments.

Cell lines	Source	Species	References
MC38	Engleman Lab Stanford University (NCI DCTD tumor/cell line repository)	Mus musculus	(90)
MC38 ^{tdTomato}	Engleman Lab Stanford University (in house)	Mus musculus	N/A
MC38 ^{ΔSTING}	This manuscript	Mus musculus	N/A
LLC	Garcia Lab Stanford University (ATCC)	Mus musculus	CLR1642
E0771	ATCC	Mus musculus	CRL-3461
RAW264.7	ATCC	Mus musculus	TIB-71
B16F1	ATCC	Mus musculus	CRL-6323

Table S3. List of critical commercial assays and reagents

Critical commercial Assays	Company	Cat#
1x Glutamine	Corning	25-005-CI
1x Penicillin/Streptomycin	Gibco	15140-122
2-Mercaptoethanol	Gibco	21985-023
4-hydroxytamoxifen	Millipore-Sigma	H6278-10MG
ACK Lysing Buffer (Gibco)	Thermo Fisher Scientific	A1049201
anhydrous acetonitrile	Thermo Fisher Scientific	271004
Anti-Biotin Microbeads	Milteni Biotec	130-090-485
BD Cytofix/Cytoperm Fixation and Permeabilization solution	BD Biosciences	554714
BD Perm/Wash™ Buffer	Fisher scientific	BD554723
Brefeldin A	Millipore-Sigma	B6542-25MG
CellTrace™ Violet Cell Proliferation Kit	Invitrogen™	C34557
Cell-ID Cisplatin	Fluidigm	201064
Collagenase D (COLLD-RO Roche)	Millipore-Sigma	11088882001
cOmplete™ EDTA-free protease inhibitor cocktail (Roche)	Millipore-Sigma	11873580001
CountBright™ Absolute Counting beads	Thermo Fisher Scientific	C36950
Corning™ EDTA (0.5M)	Corning	46034CI
Diphtheria Toxin from Corynebacterium diphtheriae	Millipore-Sigma	D0564
DMEM media	Corning	10-027-CV
DNase (Roche)	Millipore-Sigma	4716728001
DPBS (Dulbecos Phosphate Buffered Saline)	Corning	21-030-CV
Dynabeads™ Sheep Anti-Rat IgG	Thermo Fisher Scientific	11035
EDTA	Thermo Fisher Scientific	15576028
Fetal bovine Serum (FBS)	Gibco	26140079
FITC-dextran-4KDa	Millipore-Sigma	46944-500MG-F
Foxp3 Transcription Factor Fixation/Permeabilization buffer	Thermo Fisher Scientific	00-5521-00
Hank's Balanced Salt Solution (HBSS)	Corning	21-023-CV
Ionomycin calcium salt from Streptomyces conglobatus	Millipore-Sigma	I0634-5MG
Indium 115 metal chloride	Trace Sciences International	In-115
iScript Reverse Transcription Supermix	Bio-Rad	1708841
Itaq Universal SYBR	Bio-Rad	1725121
LIVE/DEAD™ Fixable Blue Dead Cell Stain Kit	Invitrogen™	L23105
Na ₃ VO ₄	Millipore-Sigma	S6508
NaCl	Fisher scientific	S271-3

NAF	Millipore-Sigma	201154
NaN3	Millipore-Sigma	769320
NanoString nCounter® Mouse Immune Exhaustion Panel V2 Standard Platforms	NanoString	115000476
NanoString nCounter® Mouse Myeloid Innate Immunity V2 Standard Platforms	NanoString	115000181
NP40	Fisher Scientific	NC9168253
Paraformaldehyde 16% aqueous solution	Electron Microscopy Sciences	15710
Phorbol 12-myristate 13-acetate (PMA)	Millipore-Sigma	P8139-1MG
Pierce™ BCA Protein Assay Kit	Thermo Fisher Scientific	23225
RPMI media	Corning	10-040-CV
Sodium-deoxycholate	Millipore-Sigma	30970
Sodium dodecyl sulfate (SDS)	Millipore-Sigma	L3771
Sodium Pyruvate Solution	Corning	25000CI
STING inhibitor (H-151)	Invivogen	inh-h151
Trypsin gold, Mass spectrometry Grade	Promega	V5280
TMTpro™ 16plex Label Reagent Set	Thermo Fisher Scientific	A44520
Tris-HCl, pH 7.4	Fisher scientific	BP152-1
VeriKine-HSTM mouse IFN beta Serum ELISA Kit	PBL assay science	42410

Table S4. List of flow cytometry antibodies

Antibody	Source	Cat#	RRID
Anti-mouse B7-H1 (MIH5) SuperBright 780	eBioscience	78-5982-82	RRID: AB_2724081
Anti-mouse CD11b (M1/70) BV650	BioLegend	101239	RRID: AB_11125575
Anti-mouse CD11b (M1/70) eFluor®450	eBioscience	48-0112	RRID: AB_1582237
Anti-mouse CD11c (HL3) BUV737	BD Biosciences	612796	RRID: AB_2870123
Anti-mouse CD11c (HL3) PE-Cy7	BD Biosciences	558079	RRID: AB_647251
Anti-mouse CD19 (6D5) Alexa Fluor® 700	BioLegend	115528	RRID: AB_493735
Anti-mouse CD19 (eBio1D3) APC-eFluor®780	eBioscience	47-0193-82	RRID: AB_10853189
Anti-mouse CD19 (eBioD3) eFluor®450	eBioscience	48-0193-82	RRID: AB_2734905
Anti-mouse CD24 (M1/69) APC-eFluor®780	eBioscience	47-0242-80	RRID: AB_10853190
Anti-mouse CD24 (M1/69) BUV395	BD Biosciences	744471	RRID: AB_2742259
Anti-mouse CD25 (PC61) PerCP Cy5.5	BioLegend	102030	RRID: AB_893288
Anti-mouse CD3e (145-2C11) APC-eFluor®780	eBioscience	47-0031-82	RRID: AB_11149861
Anti-mouse CD3e (17A2) Alexa Fluor® 700	BioLegend	100216	RRID: AB_493697
Anti-mouse CD4 (GK1.5) BUV395	BD Biosciences	563790	RRID: AB_2738426
Anti-mouse CD44 (IM7) BV785	BioLegend	103041	RRID: AB_11218802
Anti-mouse CD44 (IM7) PE-Cy7	BioLegend	103030	RRID: AB_830787
Anti-mouse CD45 (30-F11) Brilliant Violet 510™	BioLegend	103138	RRID: AB_2563061
Anti-mouse CD45 (30-F11) BV785	BioLegend	103149	RRID: AB_2564590
Anti-mouse CD45 (30-F11) FITC	BioLegend	103108	RRID: AB_312973
Anti-mouse CD45.1 (A20) FITC	eBioscience	11-0453-82	RRID: AB_465058
Anti-mouse CD45.2 (104) PE-Cy7	BioLegend	109830	RRID: AB_1186098
Anti-mouse CD64 (X54-5/7.1) APC	BioLegend	139306	RRID: AB_11219391
Anti-mouse CD8a (53-6.7) APC-eFluor®780	eBioscience	47-0081-82	RRID: AB_1272185
Anti-mouse CD8a (53-6.7) Brilliant Violet 510™	BioLegend	100751	RRID: AB_2561389
Anti-mouse CD8a (53-6.7) BUV737	BD Biosciences	564297	RRID: AB_2722580
Anti-mouse EpCAM (G8.8) PE	eBioscience	12-5791-82	RRID: AB_953615
Anti-mouse EpCAM (G8.8) PE-Cy7	eBioscience	25-5791-80	RRID: AB_1724047
Anti-mouse F4/80 (BM8) eFluor®450	eBioscience	48-4801-82	RRID: AB_1548747
Anti-mouse F4/80 (BM8) PerCP Cy5.5	BioLegend	123128	RRID: AB_893484
Foxp3 Monoclonal Antibody (FJK-16s) FITC	eBioscience	11-5773-82	RRID: AB_465243

Anti-mouse Foxp3 (FJK-16s) APC	eBioscience	17-5773-82	RRID: AB_469457
Anti-mouse IFN γ (XMG1.2) Alexa Fluor® 700	BD Biosciences	557998	RRID: AB_396979
Anti-mouse Ly6C (HK1.4) Alexa Fluor® 700	BioLegend	128024	RRID: AB_10643270
Anti-mouse Ly6C (HK1.4) eFluor®450	ebiosciences	48-5932-82	RRID: AB_10805519
Anti-mouse Ly6G (1A8) Alexa Fluor® 700	BioLegend	127622	RRID: AB_10643269
Anti-mouse MHCII (M5/114.15.2) Brilliant Violet 510™	BioLegend	107635	RRID: AB_2561397
Anti-mouse NK1.1 (PK136) Alexa Fluor® 700	BioLegend	108730	RRID: AB_2291262
Anti-mouse NK1.1 (PK136) APC-eFluor®780	eBioscience	47-5941-82	RRID: AB_2735070
Anti-mouse PD-1 (J43) Superbright 780	eBioscience	78-9985-82	RRID: AB_2734947
Anti-mouse PD-1 (J43) PE	eBioscience	12-9985-82	RRID: AB_466295
Anti-mouse SiglecH (551) APC	BioLegend	129611	RRID: AB_10643574
Anti-mouse TNF α (MP6-XT22) Brilliant Violet 650™	BioLegend	506333	RRID: AB_2562450
Anti-mouse XCR1 (ZET) FITC	BioLegend	148210	RRID: AB_2564366
Anti-mouse XCR1 (ZET) PerCP Cy5.5	BioLegend	148208	RRID: AB_2564364
Anti-mouse/human Granzyme B (GB11) Alexa Fluor® 647	BioLegend	515406	RRID: AB_2566333
Anti-mouse/human TOX (REA473) PE	Miltenyi Biotec	130-120-716	RRID: AB_2801780
Anti-mouse/human TCF1/TCF7 Alexa Fluor®488 (C63D9)	Cell Signaling Technology	6444	RRID: AB_2797627
Anti-mouse LAG-3 (C9B7W) PE-Cy7	BioLegend	125225	RRID: AB_2715763
Anti-mouse INOS (CXNFT) PE	eBioscience	12-5920-82	RRID: AB_2572642
Anti-mouse pro-IL1b (NJTEN3) PE	eBioscience	12-7114-80	RRID: AB_10736472
Anti-mouse PD-L1 (MIH5) Superbright 780	eBioscience	78-5982-82	RRID: AB_2724081
Anti-mouse CD86 (GL1) Alexa Fluor® 700	BioLegend	105023	RRID: AB_493720
Anti-mouse CD43 (S11) Alexa Fluor® 700	BioLegend	143213	RRID: AB_2800660
Anti-mouse CD62L (MEL-14) PE-Cy7	BioLegend	104418	RRID: AB_313103
Anti-mouse CD45 (30-F11) Biotin	BioLegend	103103	RRID: AB_312968

Table S5. List of CyTOF antibodies.

Antibody	Clone	Metal	Company
CD45	30-F11	Y89	Fluidigm RRID: AB_2651152
Ly6D	49-H4	CD116	BD Pharmingen RRID: AB_396664
PDCA1	927	In115	Biolegend RRID: AB_1953281
Ly6G	1A8	Pr141	Fluidigm RRID: AB_2814678
TCF4	NCI-R159-6	Nd142	Abcam RRID: AB_2714172
CD11b	M1/70	Nd143	Fluidigm RRID: AB_2811240
B220	RA3-6B2	Nd144	Fluidigm RRID: AB_2811239
MHC-II	M5/114.15.2	Nd145	Biolegend RRID: AB_2563771
EpCAM	G8.8	Nd146	Biolegend RRID: AB_2563743
CD172a	P84	Sm147	Biolegend RRID: AB_11203723
CD127	A7R34	Nd148	Biolegend RRID: AB_2563716
CD19	6D5	Sm149	Fluidigm RRID: AB_2814679
Ly6C	HK1.4	Nd150	Biolegend RRID: AB_2563783
CD64	X54-5/7.1	Eu151	Fluidigm RRID: AB_2814680
TCR beta	H57-597	Sm152	Biolegend RRID: AB_2562804
CD335 (NKp46)	29A1.4	Eu153	Biolegend RRID: AB_2563744
CD24	M1/69	Sm154	Biolegend RRID: AB_2563732
FcεR1alpha	MAR_1	Gd155	Biolegend RRID: AB_2563768
CD14	Sa14-2	Gd156	Fluidigm RRID: AB_2814681
IRF4	IRF4.3E4	Gd157	Biolegend RRID: AB_2280462
SiglecH	551	Gd158	Biolegend RRID: AB_1227757
F4/80	BM8	Tb159	Fluidigm RRID: AB_2811238
MGL2	URA-1	Gd160	Biolegend RRID: AB_2562711
CD8	53-6.7	Dy161	Biolegend RRID: AB_2562796
CD11c	N418	Dy162	Fluidigm RRID: AB_2814682
XCR1	ZET	Dy163	Biolegend RRID: AB_2563841
CCR7	4B12	Dy164	Fluidigm RRID: AB_2814683
CCR2	475301	Ho165	R&D Systems RRID: AB_10718414
CX3CR1	SA011F11	Er166	Biolegend RRID: AB_2564313
CD115	AFS98	Er167	Biolegend RRID: AB_2563709
CD116 (GMSFR)	698423	Er168	ThermoFisher Scientific RRID AB_2608189
PD-L1 (CD274)	MIH5	Tm169	Thermo Fisher Scientific RRID: AB_467781
Langerin	L31	Er170	ThermoFisher Scientific RRID AB_763454
CD103	M290	Er171	BD Pharmingen RRID: AB_394995
CD86	GL1	Yb172	Biolegend RRID: AB_313144

CD117/c-kit	2B8	Yb173	Fluidigm RRID: AB_2811230
CD135 (FLT3)	A2F10	Yb174	ThermoFisher Scientific RRID AB_467481
CADM1	3E1	Lu175	MBL RRID: AB_592783
IRF8	V3GYWCH	Yb176	ThermoFisher Scientific Custom Order

Table S6. List of Primers and custom oligos.

List of primers used for qPCR analysis, sequencing, and gRNA oligos.

Primer	Forward (5'->3')	Reverse (5'->3')
<i>Ifnb</i>	AGCTCCAAGAAAGGACGAACA	GCCCTGTAGGTGAGGTTGAT
<i>Ifna</i>	TGACCTCAACACTCAGCTCAA	AGGTGCCTGTATCTCTACCTG
<i>Isg15</i>	AGTGATGCTAGTGGTACAGAACT	CAGTCTGCGTCAGAAAGACCT
<i>Ccl2</i>	TAAAAACCTGGATCGGAACCAAA	GCATTAGCTTCAGATTTACGGGT
<i>Rpl13a</i>	ATGACAAGAAAAAGCGGATG	CTTTTCTGCCTGTTTCCGTA
<i>Cxcl10</i>	CCAAGTGCTGCCGTCATTTTC	CCAAGTGCTGCCGTCATTTTC
<i>Ccl5</i>	TTTGCCTACCTCTCCCTCG	CGACTGCAAGATTGGAGCACT
Custom gRNA oligos (5'->3')		
<i>Sting1 knockout</i>	CACCGGTCCAAGTTCGTGCGAGGCT	
<i>Sting1 knockout</i>	AAACAGCCTCGCACGAACTTGGACC	
Sanger Sequencing Primers (5'->3')		
<i>Sting1 primer_1</i>	AGGACCAGAAGGCCAAACATC	
<i>Sting1 primer_2</i>	GATGCCATACTCCAACCTGC	

Table S7. List of software and algorithms

Software and Algorithms	Source	Reference
GraphPad Prism 9	GraphPad Software, Inc.	https://www.graphpad.com/scientificsoftware/prism/
FlowJo Software v10.7.2	TreeStar, Inc.	https://www.flowjo.com/solutions/flow-jo
UMAP (Flowjo plugin)	N/A	https://github.com/lmcinnes/umap
R	N/A	https://www.R-project.org/
ggplot2 v2.2.1	N/A	https://github.com/tidyverse/ggplot2
X-shift (Flowjo plugin)	(23)	https://github.com/nolanlab/vortex
ROSALIND®	N/A	https://rosalind.bio/
ParkerICI/Premessa R package	N/A	https://github.com/ParkerICI/premessa
MSFragger (version 3.4)	N/A	https://github.com/Nesvilab/MSFragger
Fragpipe software (version 17.0)	(91)	https://github.com/Nesvilab/FragPipe